Journal of Alloys and Compounds 685 (2016) 604–609

Contents lists available at ScienceDirect

Journal of Alloys and Compounds

journal homepage: http://www.elsevier.com/locate/jalcom

Effect of kinetics on P removal by Al-Si solvent refining at low solidification temperature

Boyuan Ban [a], Xiaolong Bai [a], Jingwei Li [a], Jian Chen [a, *], Songyuan Dai [a, b]

[a] Key Laboratory of Novel Thin Film Solar Cells, Institute of Applied Technology, Hefei Institutes of Physical Science, Chinese Academy of Sciences, Hefei, 230088, China

[b] State Key Laboratory of Alternate Electrical Power System with Renewable Energy Sources, North China Electric Power University, Beijing, 102206, China

ARTICLE INFO

Article history:
Received 25 February 2016
Received in revised form
17 May 2016
Accepted 28 May 2016
Available online 30 May 2016

Keywords:
Phosphorus
Refining
Solidification
Kinetics and thermodynamics
Al-Si-P system

ABSTRACT

To determine the effect of kinetics on P removal in Al-Si-P system, three sets of experiments with different solidification temperature ranges have been carried out. High P removal rates can be confirmed. An apparent segregation coefficient is introduced to characterize the P removal in this Al-Si-P system, which are determined to be 0.0207, 0.00822 and 0.00679, when the cooling rate is 0.556 $mK \cdot s^{-1}$ and the Si contents in the melt are 39.1, 29.3, 19.4 at.%, respectively. Theoretical P contents in the primary Si phase controlled by thermodynamic factor ($\overline{X}^{T}_{P\ in\ primary\ Si}$) and theoretical P contents in the primary Si phase controlled by kinetic factor ($\overline{X}^{K}_{P\ in\ primary\ Si}$) are calculated. The results reveal that the kinetic factors have critical influence on P removal at low solidification temperature.

1. Introduction

The solar cell production, especially those based on polycrystalline Si, increases significantly with a growing demand for development of green and renewable energy. The material resource for polycrystalline Si solar cells is solar grade Si (SoG-Si). Currently, SoG-Si is mainly manufactured using the traditional Siemens process or its modified alternatives [1], which is fairly energy intensive and environment-unfriendly [2,3]. To reduce its energy consumption and pollution, new metallurgical refining processes of SoG-Si using metallurgical grade silicon (MG-Si) as a starting material have been developed, such as slag treatment [4], plasma treatment [5], vaporization refining [6] and solvent refining [7].

P is one of the major dopants in Si and should be reduced to lower than 1 ppma for solar cell application. Because the segregation coefficient of P between solid/liquid Si, 0.35 [8], is considerably much larger than those of most metallic impurities in Si, an ordinary directional solidification is not practical to remove P. On the other hand, P has high vapor pressure in molten Si [9] and can be removed from the molten Si by using vaporization refining. However, this process requires low vacuum, high holding temperature and long operation time. The high cost of the facilities and large energy consumption limit this technique from industrial application.

Solvent refining with Al-Si alloy is a very promising process to produce SoG-Si at large scale with low cost and one of the few metallurgical Si purification processes that are realized in industrial scale [10]. Compared with directional solidification of Si(1700–1800 K), solvent refining with Al-Si melt (850–1500 K) is carried out at much lower temperature, and removal of P is more efficient. The removal of P from MG-Si by solvent refining with Al-Si melt has been extensively investigated [11–13], and segregation coefficients of P between solid Si/Al-Si melt are significantly smaller than that between solid/liquid Si [14].

Our recently works have proved that kinetics [15] and trap of phosphides [16] are two very important factors controlling the removal efficiency of P at lower solidification temperature. In this work, three sets of experiments with different solidification temperature ranges have been carried out to study the effect of kinetics on P removal in the Al-Si-P system. High P removal rates can be confirmed. Macrostructure of the samples, experimental P contents in the primary Si phase and theoretical P contents in the primary Si phase controlled by the thermodynamic factor/kinetic factor with varying Si contents are studied. The results in this research show that the kinetics is the control factor of the P removal in this Al-Si-P

* Corresponding author.
E-mail address: jchen@ipp.ac.cn (J. Chen).

http://dx.doi.org/10.1016/j.jallcom.2016.05.312
0925-8388/

system, and might suggest a new method to improve the refining process of SoG-Si.

2. Experimental

To avoid the effect of other elements that may be brought in by MG-Si and commercial Al, the Al-Si alloys were prepared by mixing of high purity raw materials: Si (solar grade, 6N), Al (99.96%) and high purity Si-P master alloy. A total of 80 g raw materials were put in an alumina crucible (O.D. = 35 mm, Depth = 70 mm). The initial P content was controlled to 890 ppma in the whole sample. Three sets of experiments were carried out in this work, the parameters of each experiment are summarized in Table 1.

The experimental process was described in our previous publication [16]. The crucibles were placed in an electric resistance furnace, heated to 1473 K in Ar atmosphere, and held for 3 h. After that, the samples were cooled down quickly to 10 K above the liquidus temperature (1250 K for Al-39.1 at.% Si melt, 1123 K for Al-29.3 at% Si melt, 960 K for Al-19.4 at% Si melt) and cooled to 850 K (eutectic temperature) with a pre-determined cooling rate (0.556 $mK \cdot s^{-1}$). Then the solidified sample was taken out from the furnace and leached in diluted HCl and HNO_3. After the acid leaching, larger primary Si flakes were collected, rinsed with deionized water, dried and separated from smaller eutectic powders.

The separated primary Si flakes of each sample, which were considered as refined primary Si, were measured by sieve analysis. The macrostructure of the Al-Si alloy ingots were obtained using an optical image scanner. The chemical compositions of the primary Si flakes were tested by inductively coupled plasma optical emission spectrometrys (ICP-OES).

3. Results and discussion

3.1. Macrostructure of Al-Si ingots

Fig. 1 shows the longitudinal sections of each sample. Because the experiment is not carried out under vacuum, all the samples contain some gas bubbles in the alloy. The primary Si flakes display needle-like morphology. For the primary Si flakes concentrated near the side surface of the samples (especially in S-3), the process of the primary Si crystals growth can be seen, that is, the primary Si flakes nucleate from the margin of the alloy (cold end), then grow towards the middle of the melt until meet other primary Si flakes. The length of the primary Si flakes is about 5–10 mm. And with higher Si content, the thickness of the primary Si flakes becomes much larger.

To evaluate the size distribution and average size of the primary Si flakes, a sieve analysis can be used. Cumulative size distribution of the primary Si flakes and fineness number (*FN*) of each sample are examined. The *FN* defined by American Foundry Society, presents the average particle size along with its distribution and a larger *FN* means finer flake size. This is explained by the following Eq. (1):

$$FN = \frac{\sum_1^n (S_i \times W_i)}{\sum_1^n W_i} \tag{1}$$

where S_i is the fineness modulus of each sieve, W_i is the weight of the remaining flakes in the sieve, and n is the number of sieves.

Fig. 2(a) shows the cumulative size distribution of the primary Si flakes of each sample (mass percent). When the Si content increases, the fine flakes in the sample occupy a larger mass percent. Fig. 2(b) shows the *FN* of each sample. From sample S-1 to S-3, the *FN* decreases with increase of the Si content, which means the average size of the primary Si flakes increase with increase of the Si content. Because under higher Si content environment, more Si atoms can easily transfer to the boundary layer and build up on the growth interface.

3.2. P removal in the refined primary Si

Fig. 3(a) shows the P content in the primary Si phase from each sample examined by ICP-OES. With the increasing Si contents, the P contents in the primary Si phase fall from 21.7 ppma in sample S-1, to 8.1 ppma in sample S-2, and 6.3 ppma in sample S-3. Considering the initial P content in each sample, which is 890 ppma, relatively high P removal rates are confirmed. Because the higher Si content leads to a higher solidification temperature, these results indicate that the P removal is more effective under low solidification temperature.

During the solidification process, mass transfer in the solid Si phase occurs only by diffusion, the diffusion coefficient of P in solid Si is 3×10^{-13} cm^2/s at 1373 K, which is a quite small value compared with that of other metal elements (usually in the range of 10^{-4}~10^{-6} cm^2/s) [17]. Because of that, it can been considered as that there is no P diffusion in the solid Si phases. When a temperature gradient exists in the liquid, thermal convection will occur, because of the difference in density between cold and hot melt. Therefore, mass transfer in the liquid phase is carried out not only by diffusion but also by convection. In this case, the impurity contents in the liquid phase are partial mixing.

An apparent segregation coefficient, $k_{P\ app}$ is introduced to characterize the P removal during the whole solidification temperature range, an equation similar to Scheil equation is derived for the calculation of the solid composition as a function of f_S:

$$X_{P\ in\ primary\ Si} = k_{P\ app} X_{P\ ini} (1 - f_S)^{k_{P\ app} - 1} \tag{2}$$

where $X_{P\ in\ primary\ Si}$ is the P content (mole percentage) in the primary Si phase, $X_{P\ ini}$ is the initial P content (mole percentage) in the whole sample, and f_S is the fraction of the primary Si phase (mole percentage).

Considering that the total amount of solute in the solid must be conserved, a formula is obtained by integration of Eq. (2):

$$\int_0^{f_S} k_{P\ app} \cdot X_{P\ ini} \cdot (1 - s)^{k_{P\ app} - 1} ds = \overline{X}_{P\ in\ primary\ Si} \cdot f_S \tag{3}$$

Table 1
List of experiments.

Exp. No.	Initial Si content in whole sample (at.%)	Cooling rate ($mK \cdot s^{-1}$)	Initial P content in whole sample (ppma)
S-1	39.1	0.556	890
S-2	29.3		
S-3	19.4		

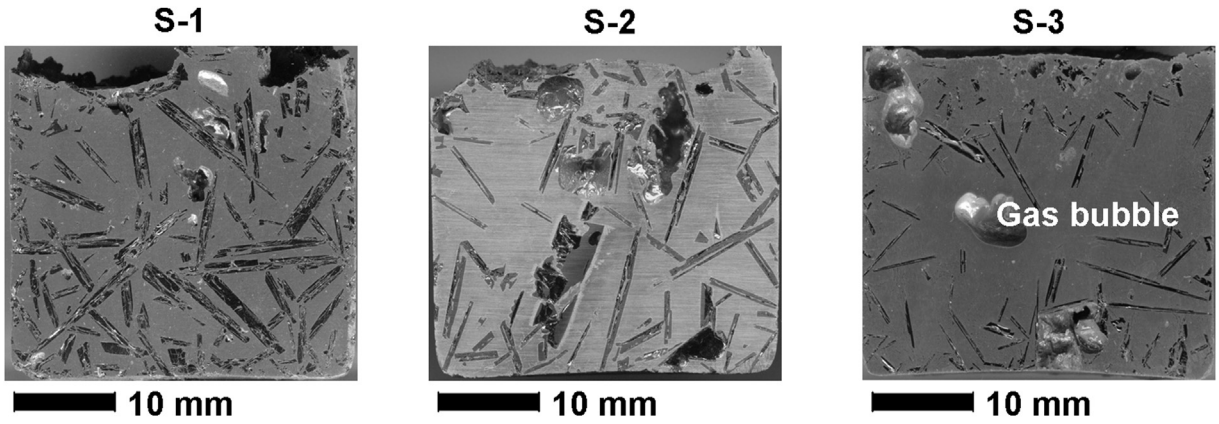

Fig. 1. Longitudinal section of samples.

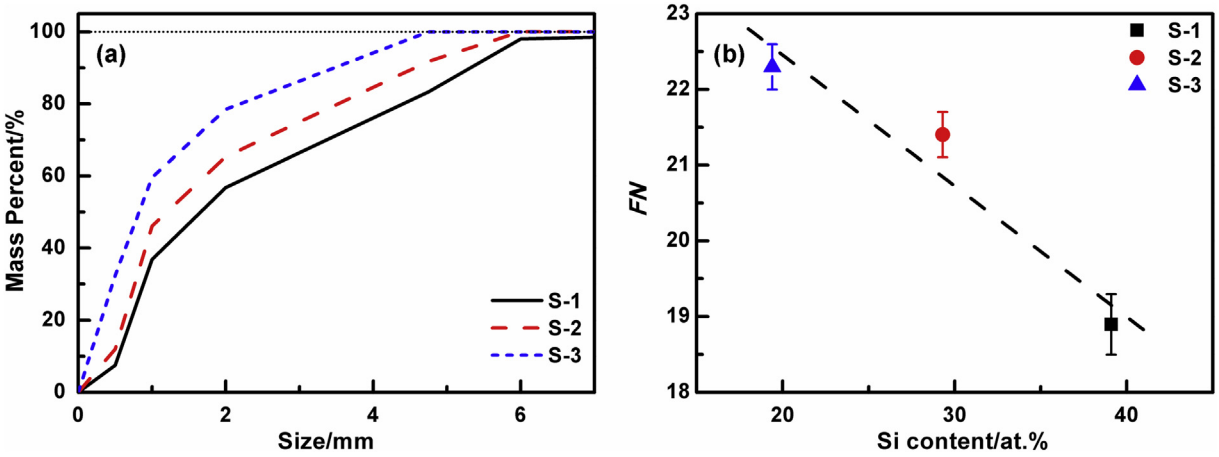

Fig. 2. (a) Cumulative size distribution of primary Si flakes in each sample, (b) *FN* of primary Si flakes in each sample.

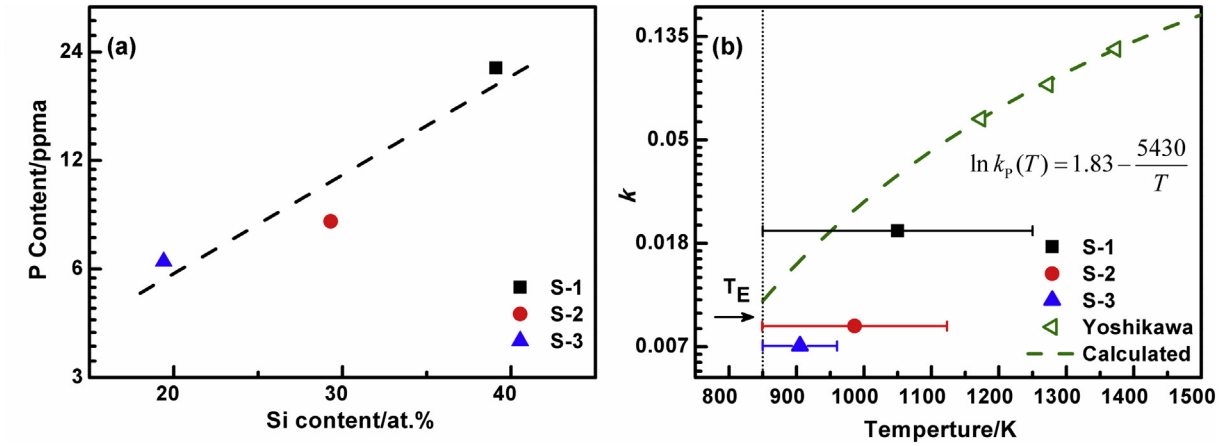

Fig. 3. (a) P content in primary Si phase from each sample, (b) k_P *vs.* $k_{P\ app}$.

$$k_{P\ app} = \log_{1-f_S}\left(1 - \frac{\overline{X}_{P\ in\ primary\ Si} \cdot f_S}{X_{P\ ini}}\right) \quad (4)$$

where $\overline{X}_{P\ in\ primary\ Si}$ is the average P content (mole percentage) in the primary Si phase obtained by ICP-OES. In this work, from Al-Si phase diagram and lever rule, f_S are 0.305, 0.195 and 0.0809 for sample S-1, S-2 and S-3 respectively, in the eutectic temperature (850 K). From Eq. (4), $k_{P\ app}$ are obtained as 0.0207 0.00822 and 0.00679 for sample S-1, S-2, and S-3, respectively.

Because the solidification is a non-isothermal process, so $k_{P\ app}$ is a parameter that is affected not only by the segregation between the solid Si phases and the Al-Si melt, but also many other factors such as mass transfer, formation of compounds, solute/particle

trapping effect. The difference between the values of $k_{P\ app}$ and the average of the segregation coefficient ($\overline{k_P}$) of the solidification temperature range shows the effect of the other factors on P removal. $\overline{k_P}$ can be written as Eq. (5):

$$\overline{k_P} = \frac{1}{T_L - T_E}\int_{T_E}^{T_L} k_P(T)\mathrm{d}T \tag{5}$$

where T_L is the liquidus temperature (1250 K for S-1, 1123 K for S-2, 960 K for S-3), T_E is the eutectic temperature of the Al-Si melt (850 K) and $k_P(T)$ is the segregation coefficient of P, which is temperature dependent. Yoshikawa et al. [14] calculated the segregation coefficient from isothermal experiment data by a least-square method, which is shown in Eq. (6).

$$\ln k_P(T) = 1.83 - \frac{5430}{T} \tag{6}$$

Substituting Eq. (6) into Eq. (5), leading to the following:

$$\overline{k_P}(S-1) = \frac{1}{1250-850}\int_{850}^{1250} exp\left(1.83 - \frac{5430}{T}\right)\mathrm{d}T = 0.0390$$

$$\overline{k_P}(S-2) = \frac{1}{1123-850}\int_{850}^{1123} exp\left(1.83 - \frac{5430}{T}\right)\mathrm{d}T = 0.0269$$

$$\overline{k_P}(S-3) = \frac{1}{960-850}\int_{850}^{960} exp\left(1.83 - \frac{5430}{T}\right)\mathrm{d}T = 0.0164$$

Compared with the $k_{P\ app}$ calculated by the experiment data, $\overline{k_P} > k_{P\ app}$, which is shown in Fig. 3(b).

The reason for this difference is mainly related to the formation of AlP particles [16]. Eq. (2) can only be used in alloys, in which the P removal is controlled by the thermodynamic factors (segregation). Whereas in this work, the kinetics might be the main controlling factors of the P removal, which is discussed in the following section.

3.3. Effect of kinetics on P removal

During the solidification process, the P removal is controlled by many factors, such as segregation, diffusion and convection in the melt, atom attachment/compounds formation, Si growth rate, solute/particle trapping effect and so on. These factors can be classified into two types: thermodynamic factor and kinetic factor. The thermodynamic factor can be seen as the P removal control factor during equilibrium solidification, which includes: complete P diffusion in the liquid phase, equilibrium segregation at the solid/liquid interface, equilibrium chemical reaction, equilibrium stable interface growth. While the kinetic factor includes mass transfer kinetic factor, crystal growth kinetic factor, reaction kinetic factor and so on.

With the assumption that the thermodynamics and the kinetics are two main factors that control the P removal, then the P content in the primary Si phase can be expressed as Eq. (7)

$$\overline{X}_{P\ \text{in primary Si}} = \overline{X}^{T}_{P\ \text{in primary Si}} + \overline{X}^{K}_{P\ \text{in primary Si}} \tag{7}$$

where $\overline{X}_{P\ \text{in primary Si}}$ is the experimental average P content in the primary Si phase obtained by ICP-OES, $\overline{X}^{T}_{P\ \text{in primary Si}}$ and $\overline{X}^{K}_{P\ \text{in primary Si}}$ are the theoretical average P content in the primary Si phase controlled by the thermodynamic factor and the kinetic factor. $\overline{X}^{T}_{P\ \text{in primary Si}}$ can be seen as the P content in the primary Si phase under equilibrium state. And $\overline{X}^{K}_{P\ \text{in primary Si}}$ can be seen as the part of P content in the primary Si phase deviated from $\overline{X}^{T}_{P\ \text{in primary Si}}$.

From the definition of segregation coefficient, the relationship of Eq. (8) can be obtained:

$$k_P(T) = \frac{X^{T}_{P\ \text{in primary Si}}}{X_{P\ \text{in Al–Si melt}}} \tag{8}$$

where $X^{T}_{P\ \text{in primary Si}}$ is the theoretical P content in the primary Si phase controlled by the thermodynamic factor and $X_{P\ \text{in Al–Si melt}}$ is the P content in the Al-Si melt, which are all temperature dependent. Considering that the total amount of solute in the solid must be conserved, the formula is obtained by integration of Eq. (8):

$$\overline{X}^{T}_{P\ \text{in primary Si}} = \frac{1}{f_S}\int_{0}^{f_S} X_{P\ \text{in Al–Si melt}} \cdot k_P(T)\mathrm{d}f \tag{9}$$

where $k_P(T)$ is the segregation coefficient of P and f is the fraction of the primary Si phase, which are all temperature dependent. And $k_P(T)$ can be obtained by Eq. (6).

H. Lescuyer et al. [18] reported that the solubility of P in Al-Si melt has the following relationship (Eq. (10)), and the Si content in the melt has no significant effect on the measured P solubility limit.

$$\log_{10}(X_{P\ \text{in Al–Si melt}}) = 0.684 - \frac{4986}{T} \tag{10}$$

Fig. 4 shows the initial P content and the P saturation curve in the Al-Si melt. As illustrated, at the melting temperature (1473 K), P is unsaturated while at the liquidus temperatures (1250 K for S-1, 1123 K for S-2, 960 K for S-3), P is saturated. $X_{P\ \text{in Al-Si melt}}$ starts from the 890 ppma, first remains constant until P is saturated and then decreases by following the P saturation curve (red arrow) until the eutectic temperature (T_E) is reached. Furthermore, $X_{P\ \text{in Al-Si melt}}$ reaches the P solubility limit before the primary Si growth, so during the solidification process, $X_{P\ \text{in Al-Si melt}}$ is a function of temperature that can be expressed by Eq. (10).

The temperature dependent fractions of solid (f) of samples are shown as Eqs. (11–13), respectively, which are calculated from Al-Si phase diagram and lever rule.

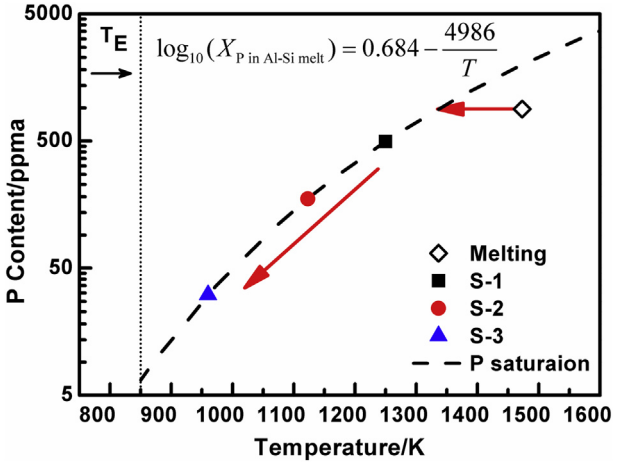

Fig. 4. Saturated P content in Al-Si melt.

$$f(\mathrm{S}-1) = 1.44 - 2.45\times10^{-3}T + 1.89\times10^{-6}T^2 - 6.85\times10^{-10}T^3 \quad (11)$$

$$f(\mathrm{S}-2) = 2.95 - 7.49\times10^{-3}T + 7.10\times10^{-6}T^2 - 2.47\times10^{-9}T^3 \quad (12)$$

$$f(\mathrm{S}-3) = 3.86 - 1.15\times10^{-2}T + 1.21\times10^{-5}T^2 - 4.55\times10^{-9}T^3 \quad (13)$$

Then df can be expressed by the following:

$$\mathrm{d}f(\mathrm{S}-1) = \left(-2.45\times10^{-3} + 3.78\times10^{-6}T - 2.06\times10^{-9}T^2\right)\mathrm{d}T \quad (14)$$

$$\mathrm{d}f(\mathrm{S}-2) = \left(-7.49\times10^{-3} + 1.42\times10^{-5}T - 7.41\times10^{-9}T^2\right)\mathrm{d}T \quad (15)$$

$$\mathrm{d}f(\mathrm{S}-3) = \left(-1.15\times10^{-2} + 2.42\times10^{-5}T - 1.36\times10^{-8}T^2\right)\mathrm{d}T \quad (16)$$

Then the range of the integral Eq. (9) is changed from 0~f_s to T_L~T_E, Eq. (9) is an integral of temperature. $\overline{X}^{T}_{P\text{ in primary Si}}$ can be calculated by substituting Eq. (6,10,14–16) into Eq. (9), The values of $\overline{X}^{T}_{P\text{ in primary Si}}$ in each sample are 9.1 ppma in S-1, 2.3 ppma in S-2, and 0.3 ppma in S-3, respectively.

Fig. 5(a) shows the relationship of $\overline{X}^{T}_{P\text{ in primary Si}}$ (Thermodyn.) and $\overline{X}_{P\text{ in primary Si}}$ (Exp.) of each sample. The ratios on the top of each column represent the percentages of $\overline{X}^{T}_{P\text{ in primary Si}}$ in $\overline{X}_{P\text{ in primary Si}}$, which are 41.92% in S-1, 28.46% in S-2, and 4.44% in S-3. Consequently, according to Eq. (7), $\overline{X}^{K}_{P\text{ in primary Si}}$ can be calculated. Fig. 5(b) shows the percentages of $\overline{X}^{K}_{P\text{ in primary Si}}$ in $\overline{X}_{P\text{ in primary Si}}$, which are 58.08% in S-1, 71.54% in S-2 and 95.56% in S-3, respectively. Because of the different solidification temperature ranges, sample S-1 is solidified at much higher temperature, and sample S-3 is solidified at lower temperature, these results indicate that the kinetic factors have critical influence on the P removal at low solidification temperature.

Our early work has proved that the formation of the AlP particles is the reason for the high P removal rates, and the AlP particles can either be trapped or pushed by the growing Si phase, which depends on the growth condition and leads to very different P contents in the refined primary Si phase. The calculation about the relationship between $\overline{X}^{T}_{P\text{ in primary Si}}$ and $\overline{X}_{P\text{ in primary Si}}$ verifies that the kinetic factors are the controlling factors of P removal in Al-Si-P system, especially at low solidification temperature. And the control power is reflected in three aspects.

1) Mass transfer kinetic factor:

During the solidification, mass transfer in the melt includes two main mechanisms: diffusion and convection. When the Si phases grow, impurities are rejected from the solid Si phases into the liquid phase. These atoms busild up in a boundary layer in the liquid just ahead of the solid/liquid (S/L) interface. In this boundary layer, the Si content decreases and the impurity content increases when the distance from the interface decreases. The diffusion mainly occurs in the boundary layer, while the convection mainly occurs in the melt. And the diffusion coefficient of P in the Al-Si melt and viscosity of the Al-Si melt are all temperature dependent:

$$D_{P\text{ in Al–Si melt}} = D_0 \exp\left(-\frac{E_a}{RT}\right) \quad (17)$$

$$\mu_{\text{Al–Si melt}} = \mu_0 \exp\left(\frac{E_b}{RT}\right) \quad (18)$$

where $D_{P\text{ in Al-Si melt}}$ and $\mu_{\text{Al-Si melt}}$ are the diffusion coefficient of P in the Al-Si melt and viscosity of the Al-Si melt, respectively. D_0 and μ_0 are coefficients, E_a and E_b are the activation energies, R is the universal gas constant. When the solidification temperature decreases, the diffusion coefficient of P in the Al-Si melt decreases and the viscosity of the Al-Si melt increases, resulting in a weakening of diffusion and convection in the Al-Si melt. Thus the liquid phase becomes partial mixing and P content in the primary Si phases increases.

2) Crystal growth kinetic factor:

Crystal growth kinetic factor mainly includes constitutional supercooling, heterogeneous nucleation, and solute/particle trapping effect. Because of the relatively slow cooling rate (0.556 mK·s^{-1}) used in this work, the growth rate is not quick enough to cause significantly degree of solute trapping effect. The

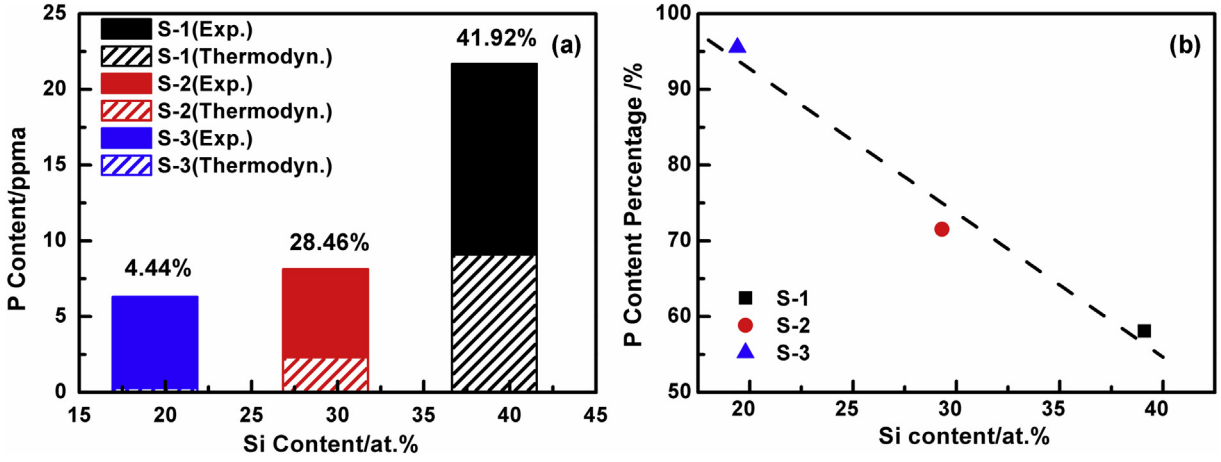

Fig. 5. (a) $\overline{X}^{T}_{P\text{ in primary Si}}$ *vs.* $\overline{X}_{P\text{ in primary Si}}$, (b) percentage of $\overline{X}^{K}_{P\text{ in primary Si}}/\overline{X}_{P\text{ in primary Si}}$.

constitutional supercooling in the interface contributes to the needle morphology of the primary Si phases shown in Fig. 1. These needle-like primary Si flakes build up a complex 3D net and separate the liquid phase into many small cells, which makes the liquid mixing much harder, resulting in the increase of P content in the primary Si phases. In this system, AlP will precipitate before the primary Si formation, and have the same space group (*Fd*-3*m*) and very similar lattice parameters (a_{Si} = 0.543 nm, a_{AlP} = 0.547 nm) [16]. Q. Han et al. [19] discussed that particles can be pushed or trapped by the growing solid, depending on the fluid flow, the size and density of the particles, the roughness of the interface and the growth rate of the solid phase. So it is very possible that the AlP particles act as the heterogeneous nuclei of Si or are trapped by the growing Si under this P over-saturated condition. This might be the main reason of the increase of P content in the primary Si phases in this Al-Si-P system.

3) Reaction kinetic factor:

The formation rate of the AlP particles is both temperature and P content dependent:

$$\frac{dc_{AlP}}{dt} = k\cdot[Al]^m\cdot[P]^n \quad (19)$$

where *m* and *n* are the reaction order of Al and P, *k* is a constant of reaction rate, [Al] and [P] are Al and P contents in the Al-Si melt. When the P content reaches a low level at lower temperature, the AlP formation rate (dc_{AlP}/dt) decreases. This causes a higher active P content in Al-Si melt under current condition than that in equilibrium state and higher P content in the primary Si phases.

The manufacture of SoG-Si using solvent refining might be improved by the mechanism discussed above. 1) From the high P removal rate in this research, the P content in the raw materials (MG-Si) is not a sensitive factor controlling the P content of the refined primary Si. This finding will greatly broaden the source of the raw materials (MG-Si) that can be used in the Si refining process and reduce the cost of the SoG-Si production. 2) Because this work is carried out at a relatively slow cooling rate (0.556 $mK\cdot s^{-1}$), the kinetic factors are still the controlling factors of the P removal in this Al-Si-P system, which indicates that only reducing the cooling rate is not an efficient method to prevent the particle trapping effect. Better processes, such as electromagnetic stirring [20,21], should be used to improve solute homogenization in the melt. These processes might avoid the AlP particles being trapped by the growing Si phase, which need more future study.

4. Conclusions

1. High removal rates of P in the refined primary Si phase are confirmed. The apparent segregation coefficients of P in this work are 0.0207 0.00822 and 0.00679 for Al-39.1 at.% Si, Al-29.3 at.% Si and Al-19.4 at.% Si, respectively.
2. Theoretical average P contents in the primary Si phase controlled by the thermodynamic factors ($\overline{X}^{T}_{P\text{ in primary Si}}$) and by the kinetic factors ($\overline{X}^{K}_{P\text{ in primary Si}}$) are calculated, the percentages of $\overline{X}^{K}_{P\text{ in primary Si}}$ in $\overline{X}_{P\text{ in primary Si}}$ are 58.08% in Al-39.1 at.% Si, 71.54% in Al-29.3 at.% Si and 95.56% in Al-19.4 at.% Si, respectively. The calculated results reveal that the kinetic factors have critical influence on P removal at low solidification temperature, which indicates that only reducing the cooling rate is not an efficient method to prevent the particle trapping effect.

Acknowledgements

This work was financially supported by "100-talent Program" of Chinese Academy of Sciences; National Natural Science Foundation of China under Grant No. 51474201, No. 51404231, Anhui Provincial Natural Science Foundation (No.1508085QE81) and China Postdoctoral Science Foundation (No. 2014M561846).

References

[1] S. Ranjan, S. Balaji, R.A. Panella, B.E. Ydstie, Silicon solar cell production, Comput. Chem. Eng. 35 (2011) 1439–1453.
[2] M.D. Johnston, L.T. Khajavi, M. Li, S. Sokhanvaran, M. Barati, High-temperature refining of metallurgical-grade silicon: a review, JOM 64 (2012) 935–945.
[3] A.F.B. Braga, S.P. Moreira, P.R. Zampieri, J.M.G. Bacchin, P.R. Mei, New processes for the production of solar-grade polycrystalline silicon: a review, Sol. Energy Mater. Sol. Cells 92 (2008) 418–424.
[4] L. Zhang, Y. Tan, J. Li, Y. Liu, D. Wang, Study of boron removal from molten silicon by slag refining under atmosphere, Mat. Sci. Semicond. Process. 16 (2013) 1645–1649.
[5] J. Wang, X. Li, Y. He, N. Feng, X. An, F. Teng, C. Gao, C. Zhao, Z. Zhang, E. Xie, Purification of metallurgical grade silicon by a microwave-assisted plasma process, Sep. Purif. Technol. 102 (2013) 82–85.
[6] N. Yuge, K. Hanazawa, K. Nishikawa, H. Terashima, Removal of phosphorus, aluminum and calcium by evaporation in molten silicon, J. Jpn. Inst. Met. 61 (1997) 1086–1093.
[7] T. Yoshikawa, K. Morita, An evolving method for solar-grade silicon production: solvent refining, JOM 64 (2012) 946–951.
[8] F.A. Trumbore, Solid solubilities of impurity elements in germanium and silicon, Bell Syst. Tech. J. 39 (1960) 205–233.
[9] T. Miki, K. Morita, N. Sano, Thermodynamics of phosphorus in molten silicon, Metall. Mater. Trans. B 27 (1996) 937–941.
[10] D. Sollmann, Pure and simple, Photon Int. 5 (2009) 110–113.
[11] T. Yoshikawa, K. Morita, Refining of silicon during its solidification from a Si-Al melt, J. Cryst. Growth 311 (2009) 776–779.
[12] J. Li, Z. Guo, H. Tang, Z. Wang, S. Sun, Si purification by solidification of Al-Si melt with super gravity, Trans. Nonferrous Met. Soc. China 22 (2012) 958–963.
[13] Y. Li, Y. Tan, J. Li, K. Morita, Si purity control and separation from Si-Al alloy melt with Zn addition, J. Alloy. Compd. 611 (2014) 267–272.
[14] T. Yoshikawa, K. Morita, Removal of phosphorus by the solidification refining with Si-Al melts, Sci. Technol. Adv. Mat. 4 (2003) 531–537.
[15] Y. Li, B. Ban, J. Li, T. Zhang, X. Bai, J. Chen, S. Dai, Effect of cooling rate on phosphorus removal during Al-Si solvent refining, Metall. Mater. Trans. B 46B (2015) 542–544.
[16] B. Ban, X. Bai, J. Li, Y. Li, J. Chen, S. Dai, The Mechanism of P Removal by solvent refining in Al-Si-P system, Metall. Mater. Trans. B 46 (2015) 2430–2437.
[17] E. Weber, Transition metals in silicon, Appl. Phys. A 30 (1983) 1–22.
[18] H. Lescuyer, M. Allibert, G. Laslaz, Solubility and precipitation of AlP in Al-Si melts studied with a temperature controlled filtration technique, J. Alloy. Compd. 279 (1998) 237–244.
[19] Q. Han, J.D. Hunt, J. Cryst. Growth 152 (1995) 221–227.
[20] B. Ban, Y. Li, Q. Zuo, T. Zhang, J. Chen, S. Dai, Refining of metallurgical grade silicon by solidification of Al-Si melt under electromagnetic stirring, J. Mater. Process. Tech. 222 (2015) 142–147.
[21] J. Jie, Q. Zou, H. Wang, J. Sun, Y. Lu, T. Wang, T. Li, Separation and purification of Si from solidification of hypereutectic Al-Si melt under rotating magnetic field, J. Cryst. Growth 399 (2014) 43–48.